Ways of Reducing Noise of a Ducted Fan Aircraft Propulsion Unit

Ing. David Hlaváček

Vedoucí práce / Thesis supervised by: doc. Ing. Luboš Janko, CSc.

Abstract

Ultralehký letoun UL-39, vyvíjený Ústavem letadlové techniky FS ČVUT v Praze, je vybaven nekonvenční ventilátorovou pohonnou jednotkou. Předkládaný příspěvek se zabývá příčinami hluku této pohonné jednotky a možnostmi jeho tlumení. Jsou zde pojmenovány a rozebrány hlavní zdroje hluku pohonné jednotky. Pro každý ze zdrojů jsou pak uvedeny vhodné metody pro výpočetní odhad akustických veličin a možné konstrukční úpravy snižující hlučnost.

The UL-39 ultra-light aircraft which is being developed by the Institute of Aerospace Engineering, Faculty of Mechanical Engineering, CTU in Prague, is equipped with an unconventional ducted fan propulson unit. This paper deals with noise sources of this propulsion unit and ways of reducing its noise level. The main sources of noise are identified and discussed. Then, for each respective source, methods of computational estimation of acoustic quantities along with potential noise-suppressing design improvements are presented.

Keywords

UL-39, ventilátorová pohonná jednotka, hluk od vzájemného působení rotoru a statoru, hluk rotoru, hluk výstupní trysky, hluk při průtoku kanály / UL-39, ducted fan propulsion unit, rotor-stator interaction noise, rotor-alone noise, cold air jet noise, flow passage noise

1 Introduction

The ducted fan propulsion unit of the UL-39 aircraft is encountering difficulties in terms of noise during its experimental operation. Beside the noise generated by the piston engine which drives the propulsion unit, tone noise generated by the fan is present in the perceived acoustic spectrum. Therefore, during its future operation, the UL-39 aircraft may not fulfill the requirements concerning noise given by legislature.

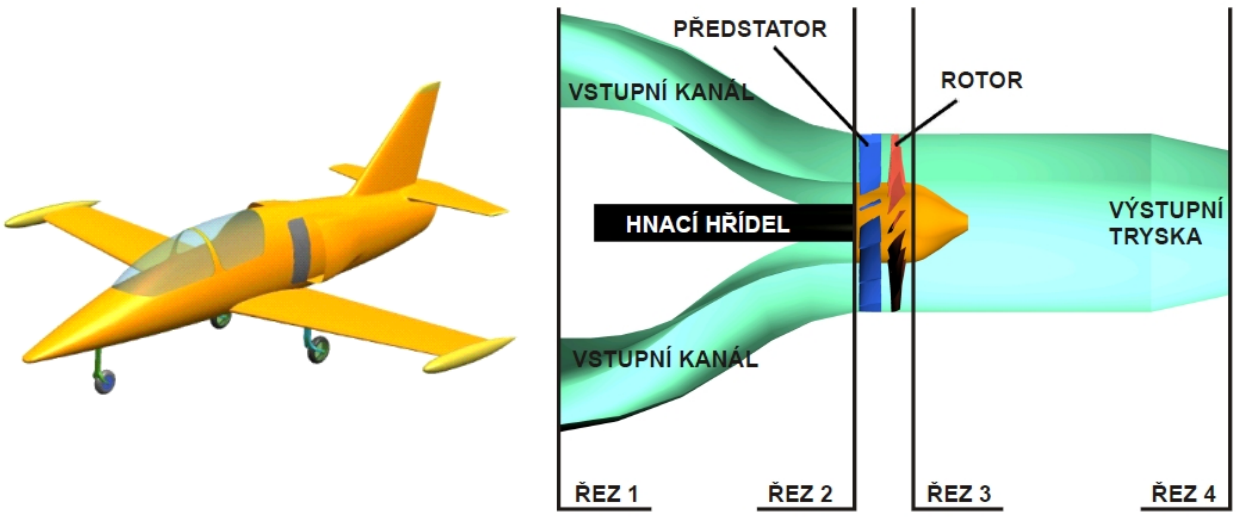

Fig. 1: The UL-39 and the arrangement of its ducted fan propulsion unit [16].

According to the project schedule, the aircraft (in its present configuration) should be able to fly in 2014. The developing team realises that if this type of progressive aircraft propulsion is to be

successful in the years to come, new goals concerning noise as well as flight dynamics will have to be set and a new model of the aircraft should be already worked on. In future, the aircraft should achieve a speed of about 300 kmph at cruise condition. The team is convinced that with the engine which is used now, the BMW S 1000 RR, this speed can be reached. However, an old fan is still coupled to the engine.

With these issues in mind, a new fan will be designed which will take into account the necessity of reducing noise while being capable to improve the aircraft flight performance at the same time.

In the following chapters, the noise sources of the propulsion unit will be identified and discussed. For each respective source, methods of computational estimation of noise level along with potential noise-suppressing design improvements will be presented. Experience from turbofan aircraft engine design as well as air-conditioning fan design will be drawn on.

2 Fan propulsion unit noise sources

Apart from the noise generated by the combustion engine (which may only be suppressed passively, that is, by insulation), four basic noise sources can be identified in the UL-39 ducted fan propulsion unit ─ the rotor-stator interaction, the rotor alone, turbulent flow inside the flow passages and the cold air jet flowing from the exit nozzle.

3 Rotor-stator interaction noise

The rotor-stator interaction generates tonal noise with a so-called blade-passing frequency which is caused by wakes behind one blade cascade interfering with another cascade placed downstream. The downstream blades generate instationary lift from which the tonal noise comes.

Methods of rotor-stator interaction noise prediction and suppression which can be applied to the UL-39 ducted fan propulsion unit were first used in turbofan engine fan design and development. Therefore, the rotor-stator configuration is only taken into account in the studies referred to. During the future development of the UL-39 propulsion unit, advantages and disadvantages of the respective fan configurations will be thoroughly discussed and the most suitable solution chosen.

3.1 Methods of rotor-stator interaction noise prediction

The instationary lift force generated by the stator blade cascade under the influence of incident wakes from rotor blades placed upstream and the resulting noise power level can be computed according to [2].

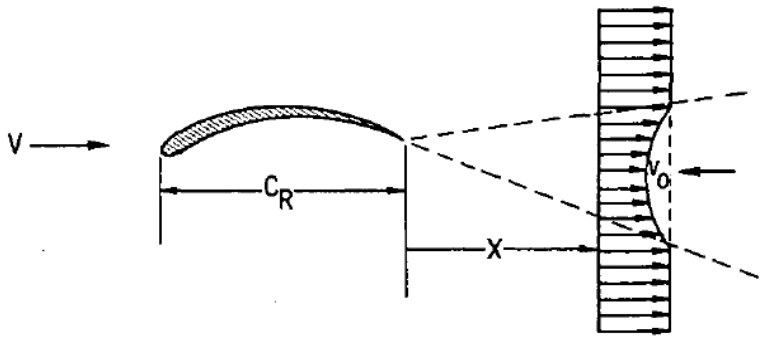

Fig. 2: Model of the rotor wake velocity defect [2].

In this technical memorandum, different equations for computing the wake velocity defect are presented and compared. With different constants, the following relationship is used:

$$\frac{v_0}{v_\infty} \sim \frac{\sqrt{c_{D,R}}}{\sqrt{\frac{x}{c_R}}} \quad . \tag{1}$$

The blade cascade drag coefficient $c_{D,R}$ is not a commonly used quantity. More often, a pressure loss coefficient is used instead:

$$\zeta_R = \frac{\Delta p_0}{\frac{1}{2}\rho w_1^2} \quad . \tag{2}$$

The following relationship exists between these two coefficients [17]:

$$c_{D,R} = \zeta_R \frac{s_R}{c_R} \cos\alpha_\infty \quad . \tag{3}$$

The response of the stator blades to the instationary pressure changes caused by the rotor wakes can be expressed using two experimentally determined functions based on the fundamentals of instationary aerodynamics, $S(\omega)$ and $T(\omega)$. These complex functions are related to transversal and longitudinal response of the stator blades, respectively (see Fig. 3).

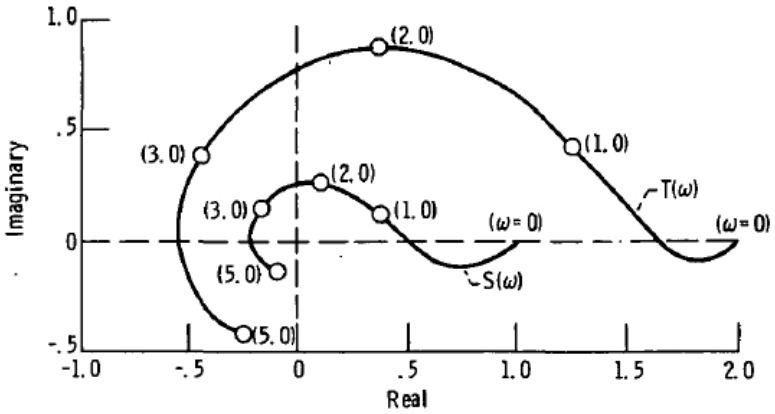

Fig. 3: Transversal and longitudinal blade response functions [2].

The change of lift generated by the stator blades under the insluience of instationarities from upstream can be determined as:

$$\Delta F_y \sim S(\omega) - \alpha T(\omega) \tag{4}$$

(the actual relationship involving a multitude of quantities is given in [2]).

The functions $S(\omega)$ and $T(\omega)$ depend on reduced frequency which is computed as follows:

$$\omega = \frac{\pi c_S z_R \Omega}{c_{a,s}} \tag{5}$$

Using this computation, no absolute noise level can be determined. However, the current fan and the new one can be compared with each other since the noise power level difference can be calculated.

$$\Delta L_W = 20 \log \frac{\Delta F_{y,2}}{\Delta F_{y,1}} \tag{6}$$

It should be noted that the above-mentioned method is not numerically precise since the equations it incorporates were derived considering a flat and isolated airfoil (not installed in a cascade). Regardless of that, it can still be used for comparing the currently-used fan to a new one.

A more sophisticated method of rotor-stator interaction noise prediction is presented in [8]. In opposition to the previous method, it is already based on a blade cascade, not an isolated airfoil.

Moreover, the cascades are assumed to be placed in a cylindrical duct of infinite length. The coordinate system used by this method is shown in Fig. 4.

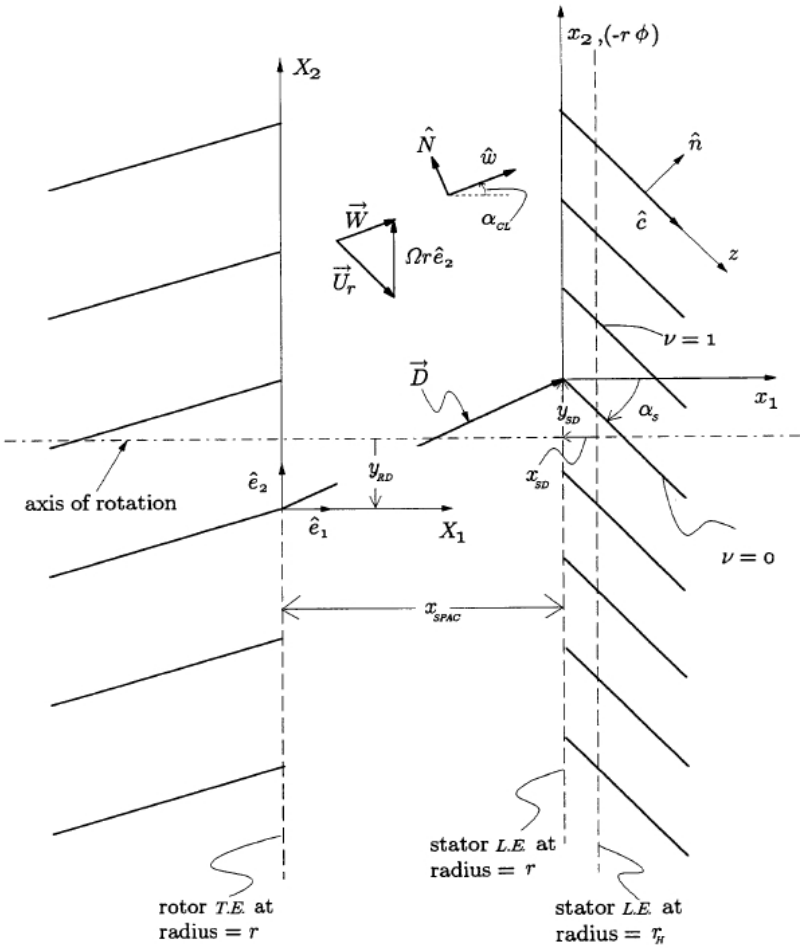

Fig. 4: Model of rotor and stator blade cascades presented in [8].

According to [8], the wakes behind the airfoils placed upstream which generate this type of noise can be modeled using various functions, including hyperbolic functions or Gaussian distribution. Recommendations concerning the wake models are presented in [9].

Using this method, the acoustic pressure field inside a cylindrical fan duct can be computed as well as noise power level generated by the fan. Since this method involves using sophisticated mathematical operations, such as Green functions or integral equations, it comes as a computer program called *V072* created by the NASA. This program is distributed via the Internet [20] on request.

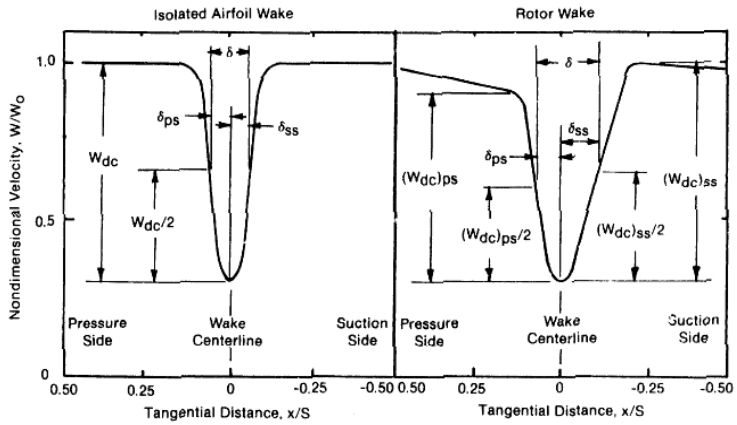

Fig. 5: Examples of wake models presented in [9].

3.2 Design improvements concerning rotor-stator interaction noise

In [2], the following methods are presented:

1. Increasing the gap between the rotor and stator. By doubling its length, a noise power level suppression of 2 dB can be achieved.

2. Changing the rotor speed. Reducing the speed may suppress the noise to a certain extent. However, the forces acting on the stator blades are greater at lower speeds which may lead to increasing the noise.

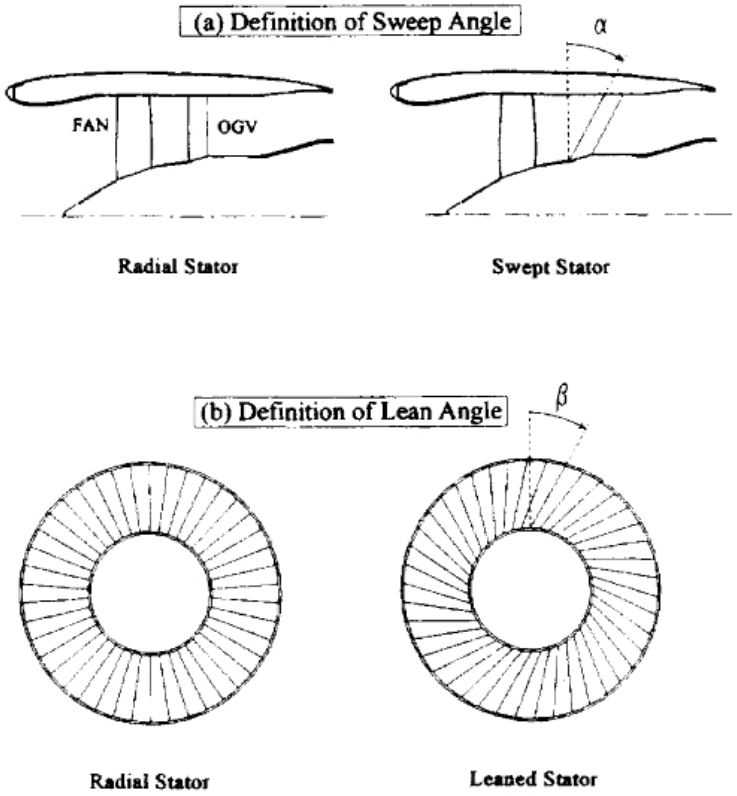

Fig. 6: The swept and leaned stator concept as presented in [4].

3. Reducing the drag coefficient of stator blades. This way, the wake velocity defect is decreased although less drag also means less lift and a therefore a smaller quantity of energy transferred by the rotor into the air flow.

4. Lenghtening the stator blades' chords. This recommendation is based on the fact that a longer chord means more wavelengths of the incident acoustic pressure waves acting on the stator blades. The incident and reflected waves can interfere and thus reduce the acoustic pressure.

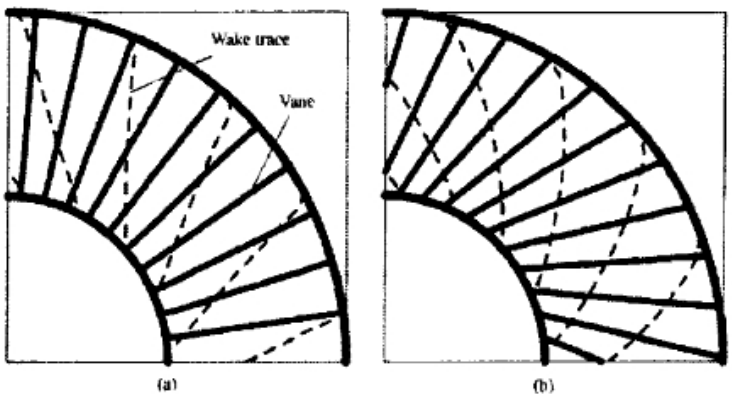

Fig. 7: Left, a stator without improvements. Right, a swept and leaned stator [5].

In [4] and [5], another noise suppression method is presented which is called the *swept and leaned stator* (see Fig. 6). The fundamental idea of this concept is increasing the number of incident wakes from the rotor blades acting on each stator blade (by leaning the stator blades) and diversifying the phase angle of these wakes at the same time (by sweeping the blades) which means that if a stator

blade is swept, the pressure waves generated by wakes in different places along the radial coordinate hit it at each at a different time. Therefore, the energy of each incident pressure wave is split into several places and moments.

As stated in [4], the swept and leaned stator can reduce the noise pressure level by 5 dB when measured in front of the engine and by 10 dB behind it.

4 Flow passage noise

4.1 Methods of flow passage noise prediction

Inside the flow passages of the ducted fan, broadband noise is generated by turbulent air flow. Its noise power level can be determined from the equation:

$$L_W = 10 + 50 \log v + 10 \log S \tag{7}$$

which is valid for straight ducts and Mach numbers usually encountered in air conditioning piping.

The noise can be suppressed by applying acoustic liners along the duct walls (which will be described below) or by reflecting the forward-radiating noise back downstream by the stator inlet guide vane (if present) or by using curved inlet channels.

The curved inlet channel (see Fig. 1) can reflect a certain part of the acoustic energy back dowstream. The value of its attenuation (denoted by D, measured in [dB]) which is a difference of acoustic power levels for the cases with and without applying noise suppressing elements, respectively, should be determined by experiment since the shape of inlet channel used in the UL-39 propulsion unit was not found in the literature studied.

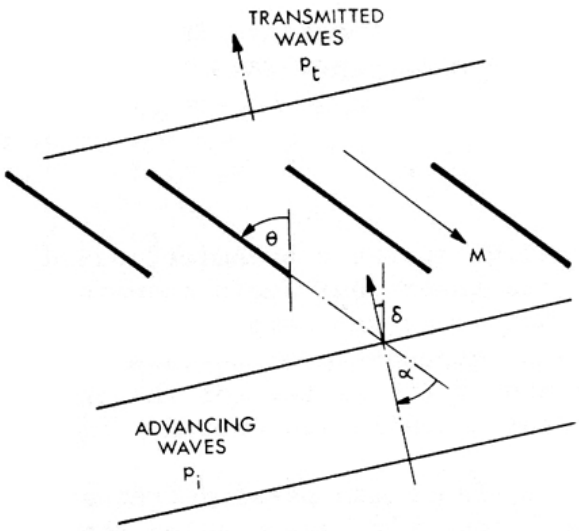

Fig. 8: The method of inlet guide vane attenuation presented in [17].

The inlet guide vane can also suppress the noise generated by the turbulent flow and the fan itself by reflection.

A method of quantifying this attenuation can be found in [17]. It is based on using the longitudinal and transversal stator blade response functions, $S(\omega)$ and $T(\omega)$, alredy mentioned above.

The calculation is to be made in elementary cylindrical layers of the fan inlet guide vane. The vane is modeled as a cascade of flat airfoils. The incident acoustic wave is assumed to be planar. A part of the incident wave (its acoustic pressure is denoted p_i) passes through the blade cascade (p_t) while the other part is reflected.

The ratio of acoustic pressures of the transmitted and incident waves is a function:

$$\frac{p_t}{p_i} = f\left(Ma_w, \alpha, \vartheta\right) \quad . \tag{8}$$

In this equation, Ma_w means the relative velocity Mach number, α is the angle between the acoustic wave direction and the blades and θ is the angle between the blades and the axis of rotation (as shown in Fig. 8).

The resulting sound attenuation can be calculated as follows:

$$D = \frac{\int_d^D \left(\frac{p_t}{p_i}\right)^2 \left(\frac{\partial F_y}{\partial t}\right)^2 \frac{1}{r} \mathrm{d}r}{\int_d^D \left(\frac{\partial F_y}{\partial t}\right)^2 \frac{1}{r} \mathrm{d}r} \tag{9}$$

The lift force time derivative can be computed using the functions $S(\omega)$ and $T(\omega)$, Mach numbers of various velocities, the blade drag coefficient and their chord length (described in [17]).

The acoustic pressure ratio is determined by calculating a system of partial differential equations. This calculation is described step by step in [7].

4.2 Design improvements concerning flow passage noise

The turbulent flow noise, along with noise from the other sources such as the driving piston engine, can be efficiently suppressed by applying acoustic liners.

Different types of acoustic liners used in aircraft propulsion are described in [3]. Two types of liners are distinghuished – locally and non-locally-acting ones.

Locally-acting liners consist of a perforated sheet, a honeycomb core, and a solid backplate. Their denomination comes from the fact that they don't allow the acoustic waves to radiate in the direction parallel to their surface. Their working principle is that of a Helmholtz resonator.

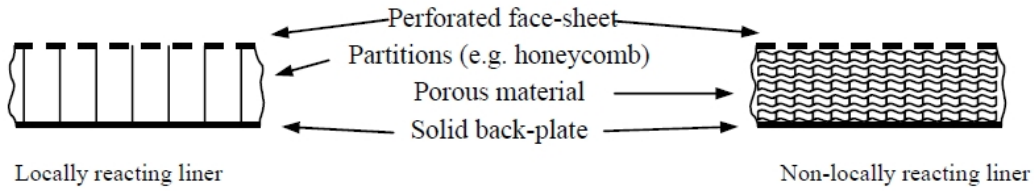

Fig. 9: Two types of acoustic liners as described in [3].

By the bandwidth of the absorbed waves, two types of locally-acting acoustic liners can be distinghuished. Single degree of freedom (SDOF) liners consist of one honeycomb layer. They only act effectively within one octave. Multiple degree of freedom (MDOF) liners are, in opposite, assembled from multiple layers of different thicknesses. These liners can absorb acoustic waves in a bandwidth of up to two octaves.

The locally-acting liners are, as already suggested, designed to absrorb acoustic waves in a relatively narrow band (which corresponds to the fan tone noise, for example). Therefore, they must be fitted for every single aircraft engine model. Their designing process is therefore long and complicated.

Non-locally-acting acoustic liners contain porous materials instead of honeycombs. They can absorb acoustic waves within a bandwidth of more than three octaves.

When applying acoustic liners to the propulsion unit if the UL-39 aircraft, the following issues are to be taken into account:

1. The complicated nature of interaction between the locally-acting acoustic liners and the surrounding flowfield prevents any simple mathematical prediction method from being applicable. However, the liners must be tuned very precisely in order to act at the frequencies needed. The fitted design of these liners, as stated above, would be so complicated as to require extensive research capacities. This already restricts the use of acoustic liners in the UL-39 propulsion unit to non-locally-acting ones.

The recent progress of research in the field of acoustic liners as well as the philosophy of the mathematical desciption of their action is further described in [3].

2. By using acoustic liners along the whole length of the duct, the weight of the aircraft would increase considerably. Moreover, the longitudinal stability conditions of the aircraft would change and would have to be calculated anew.

3. If the porous material inside the liners gets in contact with the surrounding air, it can absorb moisture or even freeze. This would further increase the weight of the aircraft.

5 Rotor-alone noise

5.1 Methods of rotor-alone noise prediction

As can be seen from the physical nature of the problem, the noise produced by the rotor itself is caused by a multitude of factors and it is not easy to predict. Not only does the rotor generate noise by its presence (and rotation) in a turbulent mean flow. It can also ingest flow instabilities from upstream or boundary layers separated from the duct walls, both of which contribute to the noise generation by locally increasing the turbulence intensity.

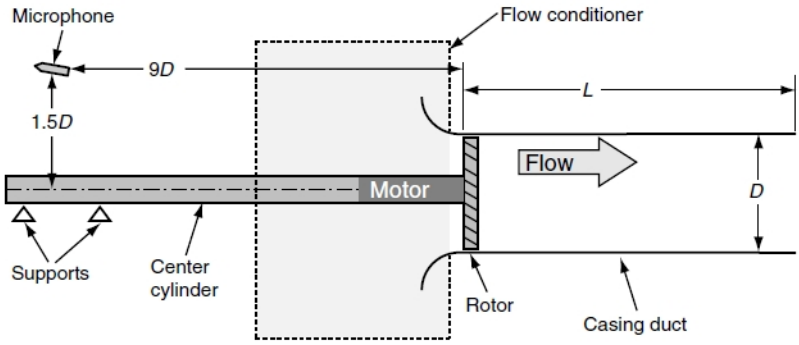

Fig. 10: A stand for rotor-alone noise measurement described in [18].

In order to separate the noise produced by the rotor itself from the other sources, a measurement was carried out which is described in [18].

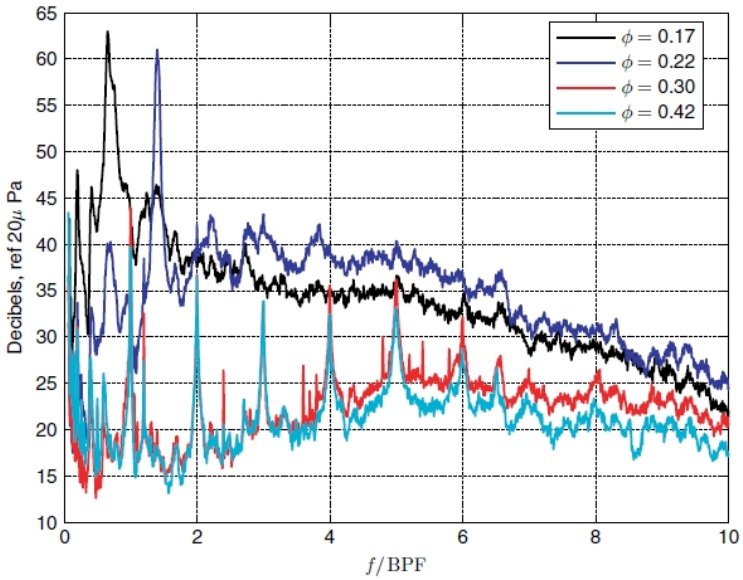

Fig. 11: Rotor acoustic spectra mesured in [18].

The arrangement of the measuring facility is shown in Fig. 10. A microphone was placed nine diameters upstream of a ducted rotor attached to an overhung end of a shaft. Using this measuring stand, a spectrum of noise pressure levels was measured at different points of the fan characteristic (Fig. 11) The respective curves are distunghuised by the Greek letter φ which stands for the

dimensionless flow rate parameter. It can be seen that the noise pressure levels increase at lower air flow rates (close to surge) due to a greater aerodynamic load acting on the blades.

This suggests that if the fan is to have improved acoustic properties, a compromise may have to be made during its design due to the fact that the best fan efficiency (as well as the greatest noise level) is usually achieved close to the surge limit.

From these results, ideas can also be made of the shape of a rotor-alone acoustic spectrum and of an experimental stand arrangement for measuring this type of noise.

Apart from that, a prediction method concerning the acoustic pressure spectral density on the surface of the rotor blades is described in [18]. The spectral density can be determined from the following integral:

$$\Phi_{\mathrm{p,R}}=\frac{z_{\mathrm{R}}c_{\mathrm{R}}}{4\pi f^2}\int_0^R U^2(r)[\Phi_{p,p}(r,f)+\Phi_{p,s}(r,f)]\,\mathrm{d}r \tag{10}$$

The functions denoted $\Phi_{\mathrm{p,p}}$ and $\Phi_{\mathrm{p,s}}$ (acoustic pressure spectral densities on the pressure and suction side of the blades, respectively) can be determined both experimentally and computationally.

The experimental evaluation of these functions is also described in [18] and involves using a miniature microphone placed inside a rotor blade close to its trailing edge (on both the pressure side and the suction side, consecutively).

The computational determination of these functions is relavitely easy and incorporates a model of a dependence of the spectral acoustic density on reduced frequency − the Goody model.

The Goody model is defined by the relationship:

$$\frac{\Phi_{\mathrm{p}}(\omega)U_{\mathrm{e}}}{\tau^2\delta}=\frac{3\omega^2}{(\omega^{0.75}+0.5)^{3.7}+(1.1\,R_{\mathrm{T}}^{-0.57}\omega)^7} \tag{11}$$

in which

$\omega=\dfrac{2\pi f\delta}{U_{\mathrm{e}}}$ stands for the reduced frequency,

δ denotes the boundary layer thickness which can be determined from the wake model shown in Fig. 5,

U_{e} is the relative velocity of the incident flow,

τ is the blade surface shear stress which can be calculated with the use of various boundary layer models,

R_{T} is a parameter respecting the Reynolds criterion. It can be calculated from the relation:

$R_{\mathrm{T}}=0.11\left(\dfrac{U_{\mathrm{e}}\vartheta}{\nu}\right)^{\frac{3}{4}}$, in which, according to [18], $\vartheta=\dfrac{\delta}{11.6}$.

These relationships are valid for both the pressure side and the suction side of the blades.

In [18], this model is compared to the experiment and it is stated that, for most cases, the results of both methods coincide to a satisfying extent (one of the results if this comparison is shown in Fig. 12).

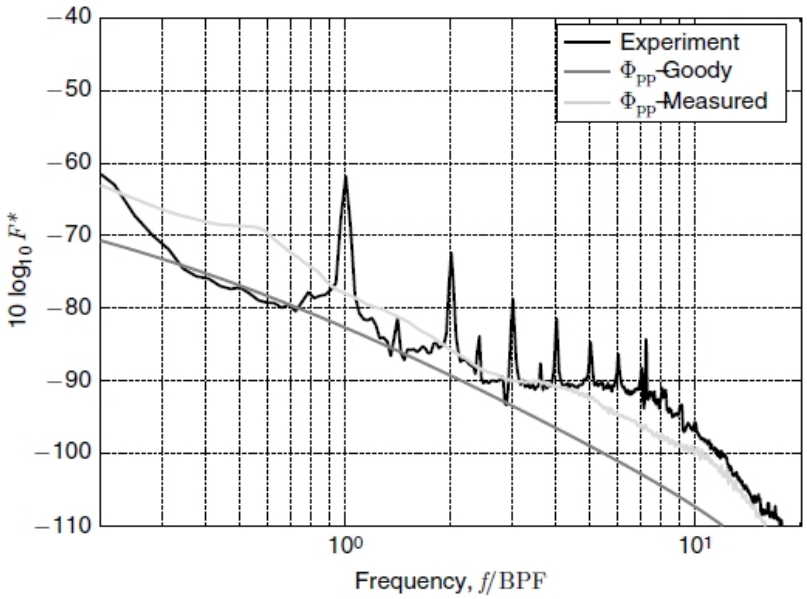

Fig. 12: The comparison of spectral acoustic densities determined by Goody model and experiment [18].

It is clear that the Goody model can be very helpful during preliminary fan design stages for comparing the currently-used fan to a new one in terms of rotor noise as well as determining the key design parameters which may help decrease this type of noise.

5.2 Design improvements concerning rotor-alone noise

One useful method of rotor noise suppression is discussed in [1]. It is based on using so-called tip platform extensions at the tips of the rotor blades.

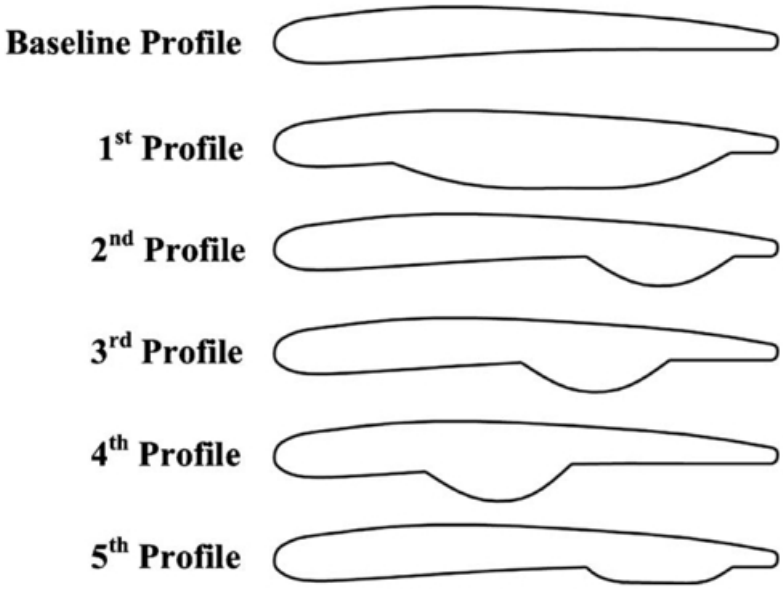

Fig. 13: Rotor tip platform extensions introduced in [1].

The fundamental idea of this improvement is reducing the generation of tip leakage vortices by preventing the air from flowing from the pressure side to the suction side of the blades to a certain extent. The vortices generated by the tip leakage flow form in a similar way to the trailing vortices behind wings of a finite span. They cause instationarities and turbulent momentum transfer in the flow which produces noise and induces aerodynamic losses inside the fan stage. Apart from the tip

leakage vortices, boundary layers at the duct walls and wakes behind the rotor blades also contribute to the resulting rotor noise.

As stated in [1], the use of tip platform extensions at the rotor blades reduces the rotor noise, widens the range of high fan efficiencies and increases its thrust. However, the contribution of the extensions to noise reduction is not quantified in [1]. The authors only claim that the best aerodynamic properties of the fan (the greatest axial velocity and, as a result, the greatest thrust) are achieved by using extensions No. 1 and 2 (shown in Fig. 13).

Fig. 14: Serrated rotor blade trailing edges as presented in [1].

Another way of suppresing rotor-alone noise which was presented in [1] is using serrated trailing edges of the rotor blades. According to [1], they should help the mixing of the wakes behind rotor airfiols with the surrounding flow. Again, their influence is not quanitified and would require measurement.

6 Cold air jet noise

6.1 Methods of cold air jet noise prediction

The acoustic power of the cold air jet flowing out of the propulsion unit's exit nozzle can be calculated using the Lighthill's equation:

$$W = K \frac{\rho D^2}{a^5} v^6 \tag{12}$$

in which

K is an experimentally determined coefficient ($K \sim 10^{-5}$), D is the nozzle exit diameter and v is the nozzle exit velocity.

This relationship is valid for Mach numbers between 0.12 and 0.5 which is the suitable range for nozzle exit speeds expected at the UL-39 propulsion unit.

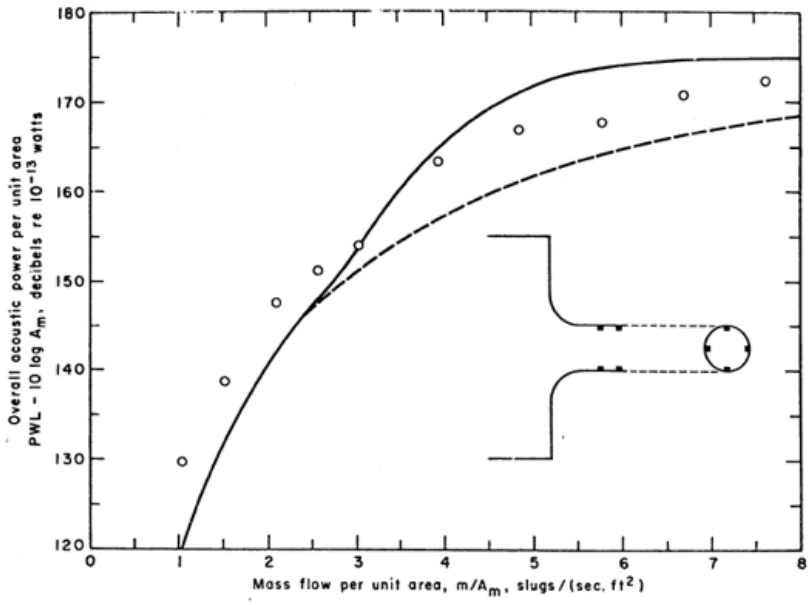

Fig. 15: A change of the acoustic power spectrum after placing screws in the exit nozzle .

From all the parameters in the above equation, the designer can influence the nozzle diameter (or, subsequentially, the nozzle exit velocity) and the coefficient *K*. This coefficient depends on the shape of the exit nozzle and the turbulence intensity of the outflowing air jet.

6.2 Design improvements concerning cold air jet

A method of cold jet noise suppression possibly applicable to the UL-39 propulsion unit can be found in [15]. Its principle is increasing the roughness of the nozzle inner walls. During an experiment presented in [15], the rough walls were simulated by screws threaded into the nozzle walls from outside. Two sets of four screws placed one after another were used, as shown in Fig. 15.

The measurements showed that after applying the screws, the acoustic power level below the choking limit of the nozzle had risen while above the choking limit, it had dropped. The acoustic power level before and after applying the screws is shown in Fig. 15. Moreover, the tone noise components disappeared completely after roughening the walls. This effect is shown in Fig. 16 (left, noise levels measured at an angle of 30° with respect to the nozzle axis, right, at 90°). Both measurements were made above the choking limit.

However, attention must be paid to the fact that, according to [13], the acoustic power level of the cold air jet strongly depends on turbulence intensity which will, of course, be increased by roughening the walls. Another issue of significance is that it is not yet certain if the nozzle will actually operate above its choking limit during flight.

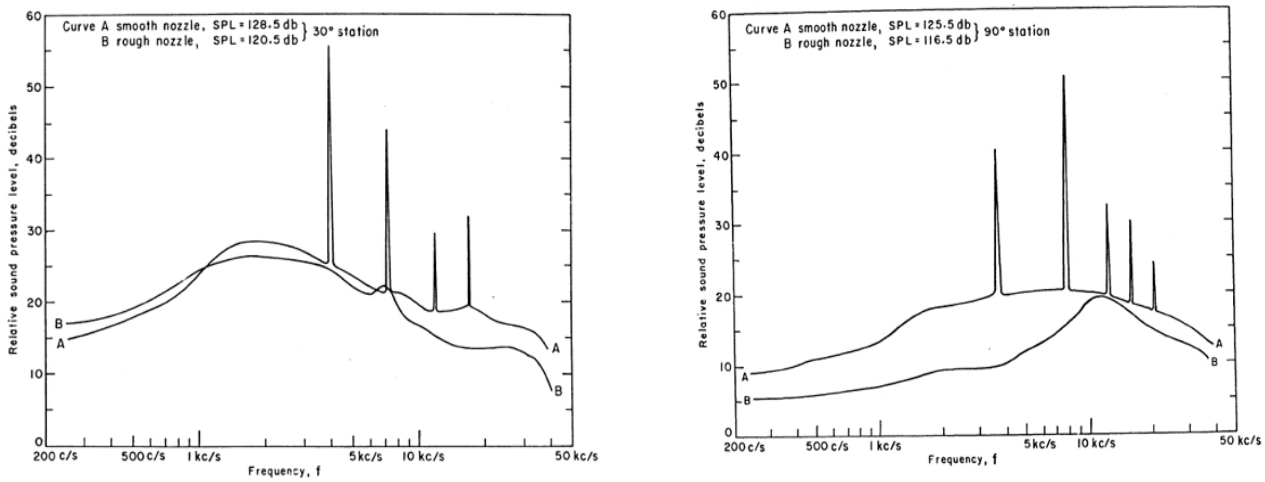

Fig. 16: The acoustic spectrum of the roughened nozzle [15].

7 Conclusions

In this paper, methods of noise prediction and suppression applicable to the UL-39 aircraft propulsion unit were presented. The respective noise sources of the propulsion unit were identified and discussed one after another.

One of the potentially most effective and, at the same time, easiest methods of noise suppression is increasing the length of stator blades and the rotor-stator gap. Sweeping and leaning the stator of the fan will be applied preferably as well. After performing the measurements needed, using rotor tip platform extensions or roughening the inner surface of the exit nozzle is also possible. Concerning the computational methods presented in this paper, all of them are relatively easy to apply and will be, of course, used during the design process.

The UL-39 developing team expects that the noise-suppressing fan design improvements will be applied subsequentially. First, the rotor-stator interaction noise along with the rotor-alone noise will be taken care of, afterwards the cold air jet noise will be an issue of interest and finally, the noise generated by the turbulent flow inside the fan duct will be suppressed. The goal of all these measures is safely adhering to the limits given by the noise legislature while maintaining sufficient properties in terms of flight dynamics of the aircraft.

List of symbols

a	speed of sound	[m.s^{-1}]
c_a	absolute flow velocity axial component	[m.s^{-1}]
$c_{D,R}$	rotor blade drag coefficient	[1]
cR	rotor blade chord length	[mm]
D	sound attenuation	[dB]
d	flow passage diameter	[mm]
f	frequency	[Hz]
F_y	lift force	[N]
K	nozzle experimental constant	[1]
L_p, L_W	noise pressure level, noise power level	[dB]
Ma	Mach number	[1]
p	pressure, acoustic pressure	[Pa]
R_T	parameter respecting the Reynolds number (Goody)	[1]
r	radial coordinate	[mm]
S	flow passage area	[m^2]
s_R	rotor blade pitch	[mm]
$S(\omega)$	stator blade transversal response function	[1]
$T(\omega)$	stator blade longitudinal response function	[1]
U, U_e	incident flow and rotor blade relative velocities	[m.s^{-1}]
u	shear velocity	[m.s^{-1}]
v	flow passage velocity, nozzle exit velocity	[m.s^{-1}]
W	acoustic power	[W]
z_R	rotor blade number	[1]
α, θ	angles	[°]
α_∞	angle of attack	[°]
Δp_0	total pressure loss	[Pa]
δ	boundary layer thickness	[mm]
ζ	pressure loss coefficient	[1]
ρ	density	[kg.m^{-3}]
τ	shear stress	[N.mm^{-2}]
Φ	acoustic pressure spectral density	[Pa.s]
Ω	rotor angular frequency	[s^{-1}]
ω	reduced angular frequency	[s^{-1}]

List of symbols

i	incident acoustic pressure
t	transferred acoutic pressure
S	stator
ss	blade suction side
ps	blade pressure side
R	rotor
w	relative flow velocity
0	wake
∞	undisturbed flow

References

[1] AKTÜRK, Ali – CAMCI, Cengiz. *Axial Flow Fan Tip Leakage Flow Control Using Tip Platform Extensions*. In: Transactions of the ASME, Vol.132, May 2010. 10 s.

[2] DITTMAR, James H. *Methods for Reducing Blade Passing Frequency Noise Generated by Rotor-wake-Stator Interaction*. Technical Memorandum. Washington: NASA, 1972. 31 s. Report No. NASA TM-X 2669.

[3] ELNADY, Tamer. *Modelling and Characterization of Perforates in Lined Ducts and Mufflers*. Doctoral Thesis. Stockholm: KTH. Department of Aeronautical and Vehicle Engineering, 2004. Supervised by Hans Bodén. 40 s.

[4] ENVIA, Edmane – NALLASAMY, M. *Design Selection and Analysis of a Swept and Leaned Stator Concept*. Technical Memorandum. Cleveland: NASA, 1998. 23 s. Report No. NASA TM-1998-208662

[5] ENVIA, Edmane. *Fan Noise Reduction: An Overview*. Technical Memorandum. Cleveland: NASA, 2001. 17 s. Report No. NASA TM-2001-210699.

[6] HUFF, Dennis L. *Fan Noise Prediction: Status and Needs*. Technical Memorandum. Cleveland: NASA, 1997. 20 s. Report No. NASA TM -97-206533.

[7] KAJI, S. – OKAZAKI, T. *Propagation of Sound Waves Through a Blade Row: I. Analysis Basedd on the Semi-actuator Disk Theory*. In: Journal of Sound and Vibration, Vol. 11, Issue 3, Mar 1970. Elsevier, 1970. 15 s. ISSN 0022-460X

[8] MEYER, Harold D. – ENVIA, Edmane. *Aeroacoustic Analysis of Turbofan Noise Generation*. Final Contractor Report. 73 s. Cleveland: NASA, 1996. Report No. NASA CR-4175.

[9] MAJJIGI, R. K. – GLIEBE, P. R. *Development of a Rotor Wake/Vortex Model. Volume I – Final Technical Report*. Final Contractor Report. Washington: NASA, 1984. 156 s. Report No. NASA CR 174849

[10] McALPINE, Alan et al. *Buzz-saw Noise: Prediction of the Rotor-alone Pressure Field*. In: Journal of Sound and Vibration, Vol. 331, Issue 22, Oct 2012. Elsevier, 2012. 18 s. ISSN 0022-460X

[11] MORAVEC, Zdeněk. *Poznámky k hluku lopatkových strojů*. Učební text postgraduálního studia "Vybrané problémy teorie, konstrukce a technologie turbinových motorů". Praha: ČVUT, 1978.

[12] MOREAU, Danielle J. – BROOKS, Laura A. – DOOLAN, Con J. *Broadband Trailing Edge Noise from a Sharp-edged Strut*. Adelaide: School of Mechanical Engineering, University of Adelaide, 2011. 30 s.

[13] NOVÝ, Richard. *Hluk a chvění*. Vydání 3. př. Praha: ČVUT, 2009. 400 s. ISBN 978-80-01-04347-9

[14] PARROTT, Tony L – JONES, Michael G – WATSON, Willie R. *Status of Duct Liner Technology for Application to Aircraft Engine Nacelles*. Conference Paper. Minneapolis: Noise-Con, 2005. 8 s.

[15] PERNET, David F. *Experimental Noise Investigation of Model Nozzles*. Technical Report. Wright-Patterson Air Force Base: Air Force Aero Propulsion Laboratory, 1964. 126 s. Report No. AFAPL-TR-64-138.

[16] POUL, Robin. *Termodynamický a aerodynamický návrh axiálního ventilátoru v uspořádání rotor-stator a předstator-rotor*. Praha: Centrum leteckého a kosmického výzkumu FS ČVUT v Praze, 2009. 50 s.

[17] SCHWARTZ, Ira R. – NAGAMATSU, Henry T. – STRAHLE, Warren C. *Aeroacoustics: Fan Noise and Control; Duct Acoustics; Rotor Noise*. Technical Papers from AIAA 2nd Aero-Acoustics Conference. New York: AIAA, Cambridge: MIT Press, 1976. 634 s. ISBN 0-915928-09-4

[18] STEPHENS, David B. – MORRIS, Scott C. *Measurements and Modeling of the Self Noise of a Low-speed Ducted Rotor*. In: Aeroacoustics volume 10, number 5&6, 2011.

[19] STONE, James R. *Interim Prediction Method for Jet Noise*. Technical Memorandum. Cleveland: NASA, 1974. 57 s. Report No. NASA TM X-71618

[20] *Glenn Research Center – Acoustics Branch Fan Tone Noise Support Home* [online]. <http://www.grc.nasa.gov/WWW/Acoustics/analysis/support/fantone.htm> c2012. [cit. 2012-11-07].